Piezotronic Effect on the Sensitivity and Signal Level of Schottky Contacted Proactive Micro/Nanowire Nanosensors

Caofeng Pan,[†,‡,§] Ruomeng Yu,[†,§] Simiao Niu,[†] Guang Zhu,[†] and Zhong Lin Wang[†,‡,*]

[†]School of Materials Science and Engineering, Georgia Institute of Technology, Atlanta, Georgia 30332-0245, United States and [‡]Beijing Institute of Nanoenergy and Nanosystems, Chinese Academy of Sciences, Beijing, China 100085. [§]These authors contributed equally to this work.

ABSTRACT We demonstrated the first piezoelectric effect on the performance of a pH sensor using an MSM back-to-back Schottky contacted ZnO micro/nanowire device. When the device is subjected to an external strain, a piezopotential is created in the micro/nanowire, which tunes the effective heights of the Schottky barriers at the local contacts, consequently increasing the sensitivity and signal level of the sensors. Furthermore, the strain-produced piezopotential along the ZnO micro/nanowire will lead to a nonuniform distribution of the target molecules near the micro/nanowire surface owing to electrostatic interaction, which will make the sensor *proactive* to detect the target molecules even at extremely low overall concentration, which naturally improves the sensitivity and lowers the detection limit. A theoretical model is proposed to explain the observed performance of the sensor using the energy band diagram. This prototype device offers a new concept for designing supersensitive and fast-response micro/nanowire sensors by introducing an external strain and piezotronic effect, which may have great applications in building sensors with fast response and reset time, high selectivity, high sensitivity, and good signal-to-noise ratio for chemical, biochemical, and gas sensing.

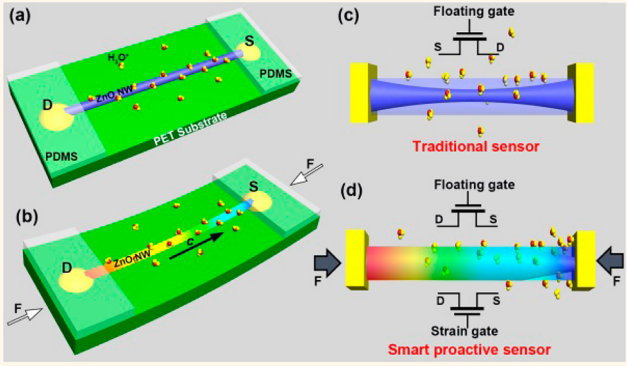

KEYWORDS: piezotronic effect · pH sensor · ZnO wires · Schottky contacted sensor

Semiconductor nanowires (NWs) are considered to be one of the most useful and diverse classes of functional nanomaterials for electronics, sensors, optoelectronics, and energy sciences, such as nanogenerators,[1−4] light-emitting diodes (LEDs),[5] nanolasers,[6] nanowire PV devices,[7−10] gas sensors,[11] biosensors,[12] and nano field-effect transistors (FETs).[5,13−16] By surface functionalization of NWs, individual NW-based FETs can serve as ultrasensitive sensors for detecting a wide range of gases, chemicals, and biomedical species.[5,12] Although the size of the devices is reduced dramatically using NWs, the sensitivity does not increase so much since the active area of the sensor decreases as well, which means the possibility of adsorbing the target molecules on the sensor surface greatly decreases as well. The largely changing resistance of the small sensors results in a rather low electric signal, usually at nA or even pA level, which normally needs advanced and expensive electronics to detect. Traditionally, in order to enhance the sensitivity, the contacts of the devices are always chosen to be ohmic for maximizing the "gating" effect from the adsorbed molecules. Also the sensor area is chosen to be so small that a group of molecules adsorbed on the surface may significantly change its conductance. In our previous work, we introduced a new approach of replacing the ohmic contact by the Schottky contact; in such a case, the contact area can be small, although the surface area of the NW can be large. Using such a design, superhigh sensitivity has been demonstrated for NW UV sensors,[17] biosensors,[18] and gas sensors.[19] The key here is that the adsorbed molecules modify the metal−semiconductor contact.

Wurtzite and zinc blend structured semiconductors, such as GaN, ZnO, CdS, and ZnSe, usually have a piezoelectric effect. Strain-induced piezoelectric polarization in the material can be effectively used to tune the semiconductor characteristics of the device,

* Address correspondence to zlwang@gatech.edu.

Received for review December 28, 2012 and accepted January 28, 2013.

Published online 10.1021/nn306007p

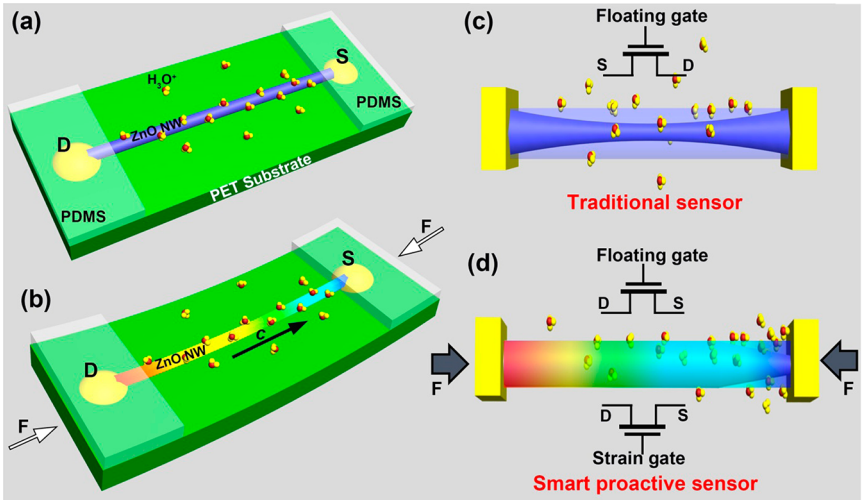

Figure 1. Schematic of the device design and working principle of a traditional NW-based FET configuration nanosensor and the piezotronics-tuned ZnO micro/nanowire proactive pH sensor. (a, b) Device design for a conventional NW sensor and the proactive sensor. (c) Working principle of the traditional NW sensor, which detects the species under the conrol of a "floating gate" introduced by the adsorption and desorption of the detected species. (d) Working principle of the ZnO micro/nanowire proactive sensor with the signal current enhanced by piezotronics effect.

which is referred to as the piezotronic effect.[20,21] Piezotronics concerns devices fabricated using the piezopotential as a "gate" voltage to tune/control charge carrier transport at a contact or junction.[22] It is demonstrated that the piezotronic effect can greatly improve the performance of photon detectors,[23] FETs,[24] and photoelectrochemical devices.[25] Here, by using a metal–semiconductor–metal (MSM) back-to-back Schottky contacted ZnO micro/nanowire device, we have demonstrated the piezoelectric effect on the performance of a pH sensor. An externally applied strain produces a piezopotential in the micro/nanowire, which tunes the effective height of the Schottky barrier at the local contact, consequently increasing the sensitivity and signal level of the sensors. Furthermore, the strain-produced piezopotential along the ZnO micro/nanowire will lead to a nonuniform distribution of the target molecules near the micro/nanowire surface owing to electrostatic interaction, which will make the sensor *proactive* to detect the target molecules even at extremely low overall concentration, which naturally improves the sensitivity and lowers the detection limit. This prototype device offers a new concept for designing supersensitive and fast-response micro/nanowire sensors by introducing the external strain and piezotronic effect, which may have great applications in building sensors with fast response and reset time, high selectivity, high sensitivity, and good signal-to-noise ratio for chemical, biochemical, and gas sensing.

RESULTS AND DISCUSSION

Working Principle. Figure 1 illustrates the working principle of a traditional NW sensor and the novel piezotronics-tuned proactive NW sensor. Traditional NW sensors typically use a functionalized NW as the essential sensor tip, which is bonded at its two ends in ohmic contacts in an FET configuration. The target molecules adsorbed on the surface of the NW may change the device's conductance by modifying the surface charges and states, disturbing the gate potential, changing the local work function and band alignment, changing the gate coupling, and/or altering the carrier mobility. We regarded these as a "floating gate" effect on the conducting channel of the FET, as shown schematically in Figure 1a and c.

The proactive sensor is based on an MSM back-to-back Schottky contacted ZnO micro/nanowire on a flexible substrate, as shown in Figure 1b and d. Due to the polarization of ions in the ZnO micro/nanowire, a piezopotential is created by applying a strain. Owing to the simultaneous possession of piezoelectricity and semiconductor properties, the piezopotential created in the crystal has a strong effect on the carrier transport at the interface/junction, known as a piezotronic effect, which tunes the effective height of the Schottky barrier (SB) asymmetrically at the local contacts and controls charge carrier transport at the contacts, consequently increasing the sensitivity and signal level of the sensors. Furthermore, the strain-produced piezopotential along the ZnO micro/nanowire will lead to a nonuniform distribution of the target molecules near the micro/nanowire surface owing to the electrostatic interaction of the local piezoelectric polarization charges with the charged molecules. Taking a pH sensor as an example, the concentration of H^+ would be higher at the negative potential end of the ZnO micro/nanowire than the average concentration in the solution due to electrostatic attraction. This will make the sensor proactive to detect the target molecules with a higher sensitivity and lower detection threshold.

Device Fabrication. The fabrication of a ZnO micro/nanowire pH sensor follows the method reported by us previously.[26] The ZnO micro/nanowire was synthesized

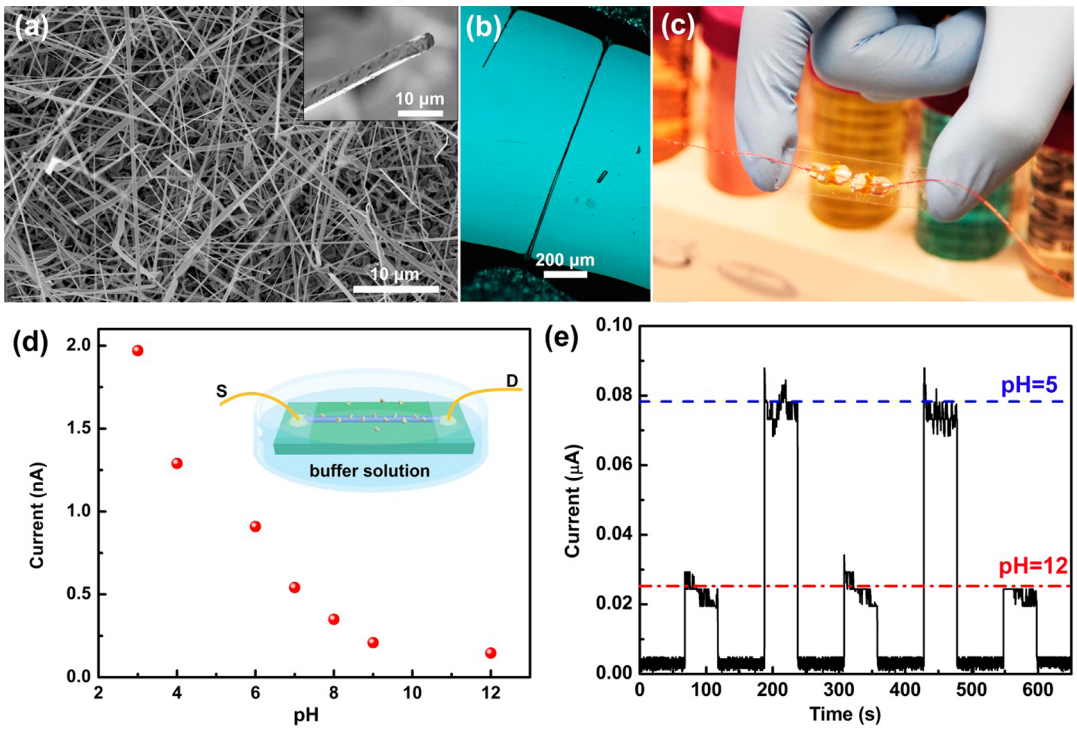

Figure 2. SEM image of the morphology of the as-synthesized ZnO micro/nanowires. The insert is a high-magnification image of an individual wire. (b, c) Optical microscopy and digital image of a ZnO micro/nanowire pH sensor. (d) Response of the sensor to the pH, varying from 3 to 12, with no external strain applied, just like traditional NW-based sensors. (e) Repeatability of the ZnO pH sensor at pH 5 and 12.

via a vapor−solid method, which gave high-quality and long micro/nanowires. The morphology of the as-fabricated ZnO micro/nanowires is presented in Figure 2a, with lengths of several hundreds of micrometers and diameters varying from tens of nanometers to several micrometers. An enlarged SEM image of an individual ZnO micro/nanowire is shown as an inset in Figure 2a. Then, a long ZnO micro/nanowire was chosen and dispersed onto a polyethylene terephthalate/or a polystyrene (PS) substrate; both ends of the ZnO micro/nanowire were fixed by silver paste, serving as electrodes as well. After that, a layer of epoxy was used to fully cover the two silver electrodes, preventing them from being exposed in the buffer solution during the following test. An optical microscopy image of an as-fabricated device is presented in Figure 2b, showing that the length of the ZnO micro/nanowire reaches over hundreds of micrometers. A real device is given in Figure 2c.

Sensor Performance Characterization. The response of the micro/nanowire sensor to the pH was tested by measuring its transportation properties in different buffer solutions. During this test, no strain was applied on the device; thus the signal level is at the nA range, just like traditional NW-based sensors. The results in Figure 2d demonstrate that the signal of the ZnO micro/nanowire sensor increased stepwise with discrete changes in pH from 12 to 3, showing a good response to the pH change. These results are controlled by the "floating gate" and can be understood by considering the surface functionality of the ZnO micro/nanowires in different buffer solutions. At low pH, H^+ is absorbed on the surface of the ZnO micro/nanowire and acts as a positive gate, which increases the electron carriers in the n-type ZnO micro/nanowire and thus increases the conductance. At high pH, OH^- is absorbed on the surface of the ZnO micro/nanowire, which correspondingly depletes the electron carriers and causes a decrease in conductance.[5] The response of the micro/nanowire sensor to the pH change is stable and repeatable (Figure 2e).

Figure 3 shows the stability and repeatability of the device under externally applied strain in different environments, such as in ambient and buffer solutions. Since the tensile strain would likely cause the failure of the ZnO micro/nanowire, only a compressive strain was applied on the device. One end of the PS substrate was fixed tightly on a manipulation holder, with the other end free to be bent. A three-dimensional (3D) mechanical stage with movement resolution of 1 μm was used to apply a strain on the free end of the PS substrate, which can be calculated according to Yang *et al.*'s work.[27] *I*−*V* characteristics of the devices at different strains in different solution (pH = 4 and 12) were recorded in Figure 3, with the *c*-axis of the ZnO wire pointing from drain to source. The insets in Figure 3a, c, and e are corresponding test conditions. We find that the device has similar behaviors when it is subjected to an external strain, either in the buffer solutions or in the ambient environment.

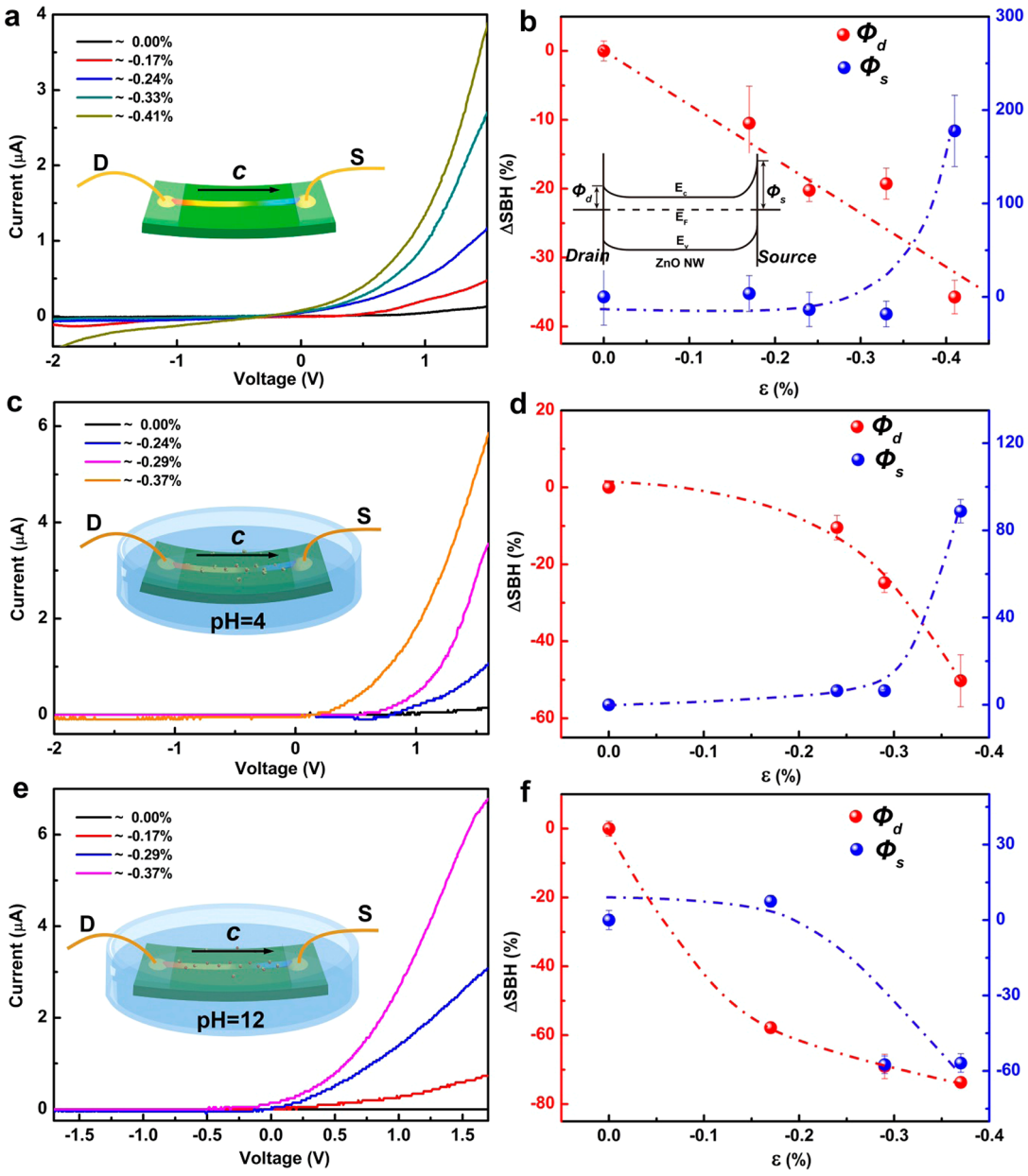

Figure 3. Stability and repeatability of the device under externally applied strain in different environments, such as in ambient and buffer solutions. (a, c, e) *I*−*V* curves of the sensor when they are under different strains when the device is in ambient air (a), in a buffer solution at pH = 4 (c), and in a buffer solution at pH = 12 (e), with the *c*-axis of the ZnO micro/nanowire parallel to the longitudinal axis of the PS substrate. The right side is the corresponding relative changes of the forward and reversely biased Schottky barrier height (ΔSBH) *vs* the applied strain extracted from the theoretical simulations corresponding to (a, c, e), respectively. An energy band diagram of such an MSM structure is presented in (b).

An energy band diagram of such an M−S−M structure is presented as insets in Figure 3b. It is clear that a compressive strain leads to a signal current increasing from nA to μA with a strain of about −0.4% applied when the device is subjected to a bias voltage of 1.5 V, which is mainly controlled by the Schottky barrier Φ_d in such an M−S−M structure.[28−31] The Schottky barrier heights Φ_d and Φ_s at the drain and source sides in Figure 3a, c, and e were quantitatively extracted through the GUI program PKUMSM developed by Peng *et al.*[29] The relative changes of the Schottky barrier heights (ΔSBH) at both sides are presented at the right-hand side of Figure 3. For such a sensor application, we mainly focus on the positive-biased *I*−*V* curves, which are determined by the Schottky barrier Φ_d, since the current is much higher than that when the sensor is negatively biased. Apparently, the trends of Φ_d in the three cases have similar behavior, which decreases with the increase in compressive strain. Usually, the trends of Φ_d and Φ_s turn out to be opposite each other due to the piezotronic effect, as presented in Figure 3b and d. Since ZnO is a piezoelectric semiconductor, a strain in the structure would produce piezocharges at the interfacial region. It

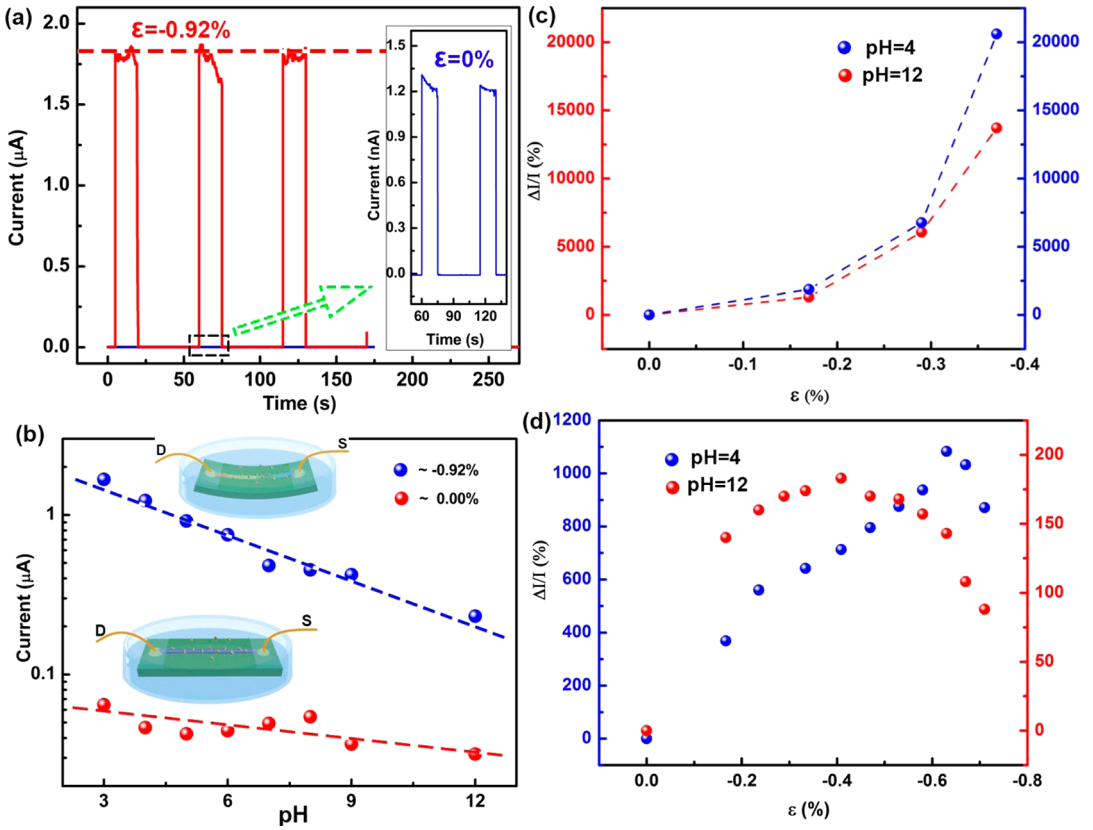

Figure 4. The signal level and the sensitivity of the sensor are increased by the piezotronics effect. (a) Output signal of a sensor in a buffer solution of pH = 5 when the strain is "off" (blue) and "on" (red). The signal is increased about 1500 times when a compressive strain of $\varepsilon = -0.92\%$ was applied. (b) Response of the sensor to the pH, varying from 3 to 12, when the device is strain off (red) and on (blue). (c, d) Relative change of the signal current responses to the strain applied on the device in the buffer solution with pH = 4 (blue) and 12 (red), respectively, which can be divided into two categories: (c) monotonically increasing, (d) with the signal current showing a maximum in response to the applied strain.

is important to note that the polarization charges are ionic charges, which are nonmobile charges located adjacent to the interface and cannot be completely canceled. The positive piezocharges may effectively lower the barrier height at the local Schottky contact, while the negative piezocharges increase the barrier height. Sometimes, the simulation program cannot get a perfect result by using the nonlinear least-squares fit to obtain these parameters. Because of this, the program drops into a local minimum, instead of a global minimum, when the source data are not very accurate, such as the current level (tens of pA) for the $I-V$ curves presented in Figure 3f, when the device is negatively biased. The performance of the device under strain in ambient and buffer solution at pH 4 and 12 shows that the device was very stable under the applied strain in different environments.

Proactive Sensor by Piezotronic Effect. The signal level of the device is increased and the sensitivity of the device is enhanced as well by the piezotronics effect, as shown in Figure 4. When a strain-free sensor was immersed in a buffer solution at pH 5, the signal level in the device was only 1.2 nA when a bias voltage of 0.5 V was applied, as the blue curve shows in the inset of Figure 4a. Thereafter, this current jumped to 1.75 μA when a compressive strain of $\varepsilon = -0.92\%$ was applied, increasing by nearly 1500 times. The responses of the ZnO micro/nanowire pH sensor to the full pH changing range when the external strain is "off" (red curve) and "on" (blue curve) are presented in Figure 4b. It indicates the same phenomenon at the full pH scale; that is, the response signal level of the device is at the nA level when the ZnO micro/nanowire is strain free, and the current response of the device is at the μA level when the ZnO micro/nanowire is compressively strained to $\varepsilon = -0.92\%$. The piezotronic effect can not only increase the signals level of the sensor but can also increase the sensitivity, which can be extracted from the slope of the current–pH relationship in Figure 4b. A larger slope means higher sensitivity and better selectivity for the pH sensor.

The piezotronic effect increases the signal level of the device and enhances the sensitivity of the device by tuning the effective heights of the two SBs and thus the characteristic of the NW sensor. The decrease of the Φ_d increases the signal current level, while the increase of the Φ_s decreases the signal current. As a result, two kinds of characteristic relationships between the sensor performance and the applied strain have been observed. The first one is that the signal current

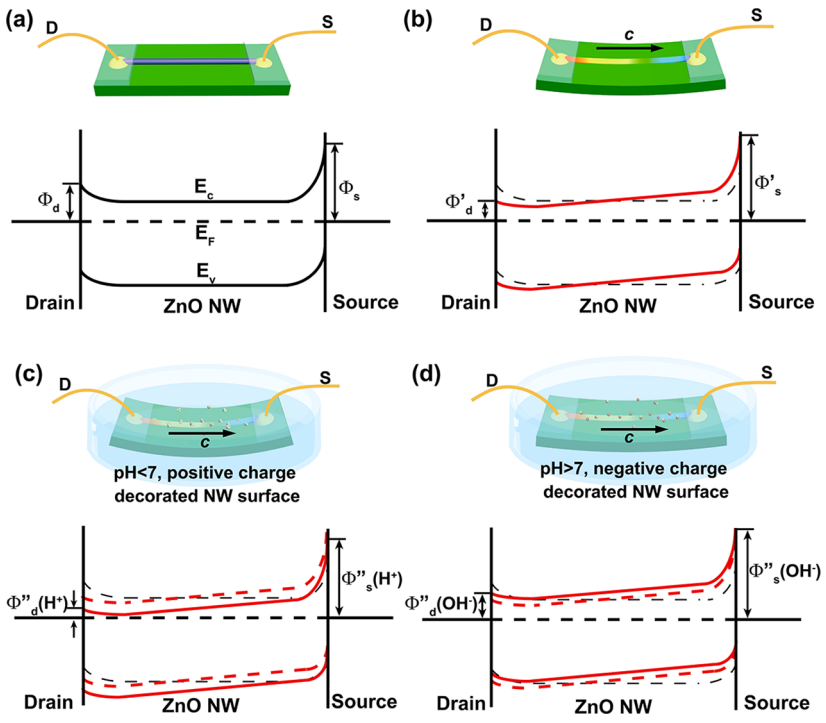

Figure 5. Schematic energy band diagrams illustrating the asymmetric Schottky barriers at the source and drain contacts (a) unstrained, (b) compressively strained in air, (c) compressively strained in an acid buffer solution, and (d) compressively strained in a buffer solution with pH greater than 7.

increases with applied strain, as shown in Figure 4c, showing the stepwise monotonically increasing signal current from the nA to μA range at pH = 4 (red curve) and 12 (blue curve). In the second case, the signal current shows a maximum in responding to the applied strain.

Theoretical Model. A theoretical model is proposed to explain the piezotronic effect on the performance of the pH sensors using energy band diagrams, as shown in Figure 5. For piezoelectric semiconductors such as ZnO and GaN, a piezoelectric potential is created inside the NW by applying a strain/pressure/force owing to the noncentral symmetric crystal structure.[2] Once a strain is created in the ZnO micro/nanowire, there exists a piezopotential distribution along the *c*-axis (the micro/nanowire direction). The role played by the piezopotential is to effectively change the local contact characteristics through an internal field; thus, the charge carrier transport process is tuned at the metal−semiconductor contact. For n-type materials, a negative piezopotential effectively increases the local SBH, while a positive piezopotential reduces the barrier height.

When the ZnO micro/nanowire device is under compressive strain, as shown in Figure 5b, the source has a negative piezopotential and thus an increase in the SBH, while the drain has a positive piezopotential with a lowed SBH. When a low compressive strain is applied, the SBH Φ_s is not very high; the transport property of the sensor is dominated by the SBH Φ_d, as shown in Figure 4c. However, with a continuous increase in compressive strain, the SBH Φ_s is even further increased, which starts to hinder the transport property of the electrons, resulting in a decrease in electric current. Therefore, there exists a critical strain value at which the transported current of the entire device reaches the optimum, as shown in Figure 4d.

The volume effect of the floating gate, which is much weaker than the strain gated piezotronic effect at the interface, can be understood by considering the surface charge states of the ZnO micro/nanowires in different buffer solutions. At low pH (Figure 5c), H^+ is absorbed on the surface of the ZnO micro/nanowire and acts as a positive "gate", which is equivalent to simultaneously lowering the conduction and valence bands of ZnO, as labeled in Figure 5c, resulting in a decrease of the bands including the heterojunction interface to lower energy, thus increasing the conductance. At a high pH, OH^- is adsorbed on the surface of the ZnO micro/nanowire, correspondingly depleting the electron carriers, which is equivalent to increasing all bands of ZnO, as labeled in Figure 5d, and causing a decrease in conductance. That is to say, the conduction and valence bands of the ZnO micro/nanowire are lower in a low pH solution than that in a high pH solution. This is the reason that the maximum point occurs at a higher strain for pH = 4 than that for pH = 12 (see Figure 4d).

Discussion. Different from traditional NW sensors, our ZnO micro/nanowire sensor is a proactive-type sensor. The strain-produced piezopotential along the

ZnO micro/nanowire will lead to a nonuniform distribution of the target molecules near the NW surface. Taking the pH sensor as an example, the concentration of H^+ would be higher at the negative potential end of the ZnO micro/nanowire than the average concentration in the solution. This means that such a piezopotential can enable a ZnO micro/nanowire sensor to detect a concentration even below the detection limit of the sensor without being strained. Furthermore, by increasing the signal level of the entire device from nA to μA without sacrificing the sensitivity, the need to utilize advanced electronics for measuring the signal will be avoided, which is beneficial for the commercialization of the technology.

Lastly, we discuss the stability of the ZnO micro/nanowires in chemical solution. A GaN NW is a better choice for building such a piezotronic effect tuned proactive sensor, due to its excellent chemical stability in buffer solutions. But the cost is very high of GaN NWs replacing the ZnO micro/nanowires, since GaN NWs are always synthesized *via* high-cost MOCVD or MBE methods. On the contrary, a ZnO micro/nanowire is a very economic choice and can be easily obtained *via* many methods, such as the hydrothermal method, chemical vapor deposition, physical vapor deposition, and so on. Although ZnO cannot sustain long-time immersion in very low pH or very high pH buffer solutions, the device was stable during our test, which is nearly 4 h for each experiment. In a practical application, the pH sensor would not be required to work continuously in the buffer solution; rather a few seconds would be enough. This means that a ZnO micro/nanowire sensor can be repeatedly used for a few thousand times. For these above-mentioned reasons, a ZnO micro/nanowire is a good choice for building a prototype of such proactive sensors.

CONCLUSION

In summary, we demonstrated the first piezotronic effect on the performance of a pH sensor using an MSM back-to-back Schottky contacted ZnO micro/nanowire device. When the device is subjected to an external strain, a piezopotential is created in the NW, which tunes the effective heights of the Schottky barriers at the local contacts, consequently increasing the sensitivity and signal level of the sensors. A theoretical model is proposed to explain the observed performance of the sensor using the energy band diagram. This study has a bright future for applications in building sensors with fast response and reset times, high selectivity, high sensitivity, and good signal-to-noise ratio.

METHODS

ZnO Micro/Nanowire Synthesis and Device Fabrication. ZnO micro/nanowires were fabricated *via* the vapor−solid growth process. ZnO powder was placed in the center of the tube furnace, while the alumina substrate was placed 25 cm downstream from the center. The typical synthesis was carried out at a temperature of 1400 °C and pressure of 75 Torr for 3 h.

The fabrication of a ZnO micro/nanowire pH sensor follows the procedure repoted by us previously.[26] A bundle of surface-functionalized wires were "picked up" or scratched onto the substrate. Then checking the wires with an optical microscope, a long and separated ZnO micro/nanowire was chosen. In this step, wires can be easily distinguished with an optical microscope with a magnification around 100×. Then both ends of the ZnO micro/nanowire were fixed by silver paste, serving as electrodes as well. After that, a layer of epoxy was used to fully cover the two silver electrodes, preventing them from being exposed to the buffer solution during the following test.

Piezotronic Effect on ZnO Micro/Nanowire pH Sensors. One end of the PS substrate was fixed tightly on a manipulation holder, with the other end free to be bent. A 3D mechanical stage with movement resolution of 1 μm was used to apply a strain on the free end of the PS substrate. $I-V$ characteristics of the devices at different strains in solution with different pH's were recorded.

Conflict of Interest: The authors declare no competing financial interest.

Acknowledgment. This research was supported by the Airforce, MURI, U.S. Department of Energy, Office of Basic Energy Sciences (DE-FG02-07ER46394), NSF, and the Knowledge Innovation Program of the Chinese Academy of Sciences (KJCX2-YW-M13).

REFERENCES AND NOTES

1. Wang, X. D.; Song, J. H.; Liu, J.; Wang, Z. L. Direct-Current Nanogenerator Driven by Ultrasonic Waves. *Science* **2007**, *316*, 102–105.
2. Wang, Z. L.; Song, J. H. Piezoelectric Nanogenerators Based on Zinc Oxide Nanowire Arrays. *Science* **2006**, *312*, 242–246.
3. Pan, C. F.; Guo, W. X.; Dong, L.; Zhu, G.; Wang, Z. L. Optical Fiber-Based Core-Shell Coaxially Structured Hybrid Cells for Self-Powered Nanosystems. *Adv. Mater.* **2012**, *24*, 3356–3361.
4. Pan, C. F.; Li, Z. T.; Guo, W. X.; Zhu, J.; Wang, Z. L. Fiber-Based Hybrid Nanogenerators for/as Self-Powered Systems in Biological Liquid. *Angew. Chem., Int. Ed.* **2011**, *50*, 11192–11196.
5. Cui, Y.; Lieber, C. M. Functional Nanoscale Electronic Devices Assembled Using Silicon Nanowire Building Blocks. *Science* **2001**, *291*, 851–853.
6. Huang, M. H.; Mao, S.; Feick, H.; Yan, H. Q.; Wu, Y. Y.; Kind, H.; Weber, E.; Russo, R.; Yang, P. D. Room-Temperature Ultraviolet Nanowire Nanolasers. *Science* **2001**, *292*, 1897–1899.
7. Pan, C. F.; Luo, Z. X.; Xu, C.; Luo, J.; Liang, R. R.; Zhu, G.; Wu, W. Z.; Guo, W. X.; Yan, X. X.; Xu, J.; *et al.* Wafer-Scale High-Throughput Ordered Arrays of Si and Coaxial $Si/Si_{1-x}Ge_x$ Wires: Fabrication, Characterization, and Photovoltaic Application. *ACS Nano* **2011**, *5*, 6629–6636.
8. Tian, B. Z.; Zheng, X. L.; Kempa, T. J.; Fang, Y.; Yu, N. F.; Yu, G. H.; Huang, J. L.; Lieber, C. M. Coaxial Silicon Nanowires as Solar Cells and Nanoelectronic Power Sources. *Nature* **2007**, *449*, 885–U8.
9. Kempa, T. J.; Tian, B. Z.; Kim, D. R.; Hu, J. S.; Zheng, X. L.; Lieber, C. M. Single and Tandem Axial p-i-n Nanowire Photovoltaic Devices. *Nano Lett.* **2008**, *8*, 3456–3460.
10. Pan, C. F.; Niu, S. M.; Ding, Y.; Dong, L.; Yu, R. M.; Liu, Y.; Zhu, G.; Wang, Z. L. Enhanced Cu_2S/CdS Coaxial Nanowire Solar Cells by Piezo-Phototronic Effect. *Nano Lett.* **2012**, *12*, 3302–3307.
11. Comini, E.; Faglia, G.; Sberveglieri, G.; Pan, Z. W.; Wang, Z. L. Stable and Highly Sensitive Gas Sensors Based on Semiconducting Oxide Nanobelts. *Appl. Phys. Lett.* **2002**, *81*, 1869–1871.

12. Patolsky, F.; Zheng, G. F.; Lieber, C. M. Nanowire-Based Biosensors. *Anal. Chem.* **2006**, *78*, 4260–4269.
13. Duan, X. F.; Huang, Y.; Cui, Y.; Wang, J. F.; Lieber, C. M. Indium Phosphide Nanowires as Building Blocks for Nanoscale Electronic and Optoelectronic Devices. *Nature* **2001**, *409*, 66–69.
14. Arnold, M. S.; Avouris, P.; Pan, Z. W.; Wang, Z. L. Field-Effect Transistors Based on Single Semiconducting Oxide Nanobelts. *J. Phys. Chem. B* **2003**, *107*, 659–663.
15. Patolsky, F.; Zheng, G.; Lieber, C. M. Nanowire Sensors for Medicine and the Life Sciences. *Nanomedicine (London, U. K.)* **2006**, *1*, 51–65.
16. Patolsky, F.; Zheng, G. F.; Hayden, O.; Lakadamyali, M.; Zhuang, X. W.; Lieber, C. M. Electrical Detection of Single Viruses. *Proc. Natl. Acad. Sci. U. S. A.* **2004**, *101*, 14017–14022.
17. Zhou, J.; Gu, Y. D.; Hu, Y. F.; Mai, W. J.; Yeh, P. H.; Bao, G.; Sood, A. K.; Polla, D. L.; Wang, Z. L. Gigantic Enhancement in Response and Reset Time of ZnO UV Nanosensor by Utilizing Schottky Contact and Surface Functionalization. *Appl. Phys. Lett.* **2009**, *94*, 191103.
18. Yeh, P. H.; Li, Z.; Wang, Z. L. Schottky-Gated Probe-Free ZnO Nanowire Biosensor. *Adv. Mater.* **2009**, *21*, 4975–4978.
19. Wei, T. Y.; Yeh, P. H.; Lu, S. Y.; Lin-Wang, Z. Gigantic Enhancement in Sensitivity Using Schottky Contacted Nanowire Nanosensor. *J. Am. Chem. Soc.* **2009**, *131*, 17690–17695.
20. Wang, Z. L. Piezopotential Gated Nanowire Devices: Piezotronics and Piezo-phototronics. *Nano Today* **2010**, *5*, 540–552.
21. Wang, Z. L. Piezotronic and Piezophototronic Effects. *J. Phys. Chem. Lett.* **2010**, *1*, 1388–1393.
22. Wang, Z. L. Progress in Piezotronics and Piezo-Phototronics. *Adv. Mater.* **2012**, *24*, 4632–4646.
23. Liu, Y.; Yang, Q.; Zhang, Y.; Yang, Z. Y.; Wang, Z. L. Nanowire Piezo-phototronic Photodetector: Theory and Experimental Design. *Adv. Mater.* **2012**, *24*, 1410–1417.
24. Liu, W. H.; Lee, M.; Ding, L.; Liu, J.; Wang, Z. L. Piezopotential Gated Nanowire-Nanotube Hybrid Field-Effect Transistor. *Nano Lett.* **2010**, *10*, 3084–3089.
25. Starr, M. B.; Shi, J.; Wang, X. D. Piezopotential-Driven Redox Reactions at the Surface of Piezoelectric Materials. *Angew. Chem., Int. Ed.* **2012**, *51*, 5962–5966.
26. Xu, S.; Qin, Y.; Xu, C.; Wei, Y. G.; Yang, R. S.; Wang, Z. L. Self-Powered Nanowire Devices. *Nat. Nanotechnol.* **2010**, *5*, 366–373.
27. Yang, R. S.; Qin, Y.; Dai, L. M.; Wang, Z. L. Power Generation with Laterally Packaged Piezoelectric Fine Wires. *Nat. Nanotechnol.* **2009**, *4*, 34–39.
28. Yu, R. M.; Dong, L.; Pan, C. F.; Niu, S. M.; Liu, H. F.; Liu, W.; Chua, S.; Chi, D. Z.; Wang, Z. L. Piezotronic Effect on the Transport Properties of GaN Nanobelts for Active Flexible Electronics. *Adv. Mater.* **2012**, *24*, 3532–3537.
29. Liu, Y.; Zhang, Z. Y.; Hu, Y. F.; Jin, C. H.; Peng, L. M. Quantitative Fitting of Nonlinear Current-Voltage Curves and Parameter Retrieval of Semiconducting Nanowire, Nanotube and Nanoribbon Devices. *J. Nanosci. Nanotechnol.* **2008**, *8*, 252–258.
30. Han, X. D.; Zheng, K.; Zhang, Y. F.; Zhang, X. N.; Zhang, Z.; Wang, Z. L. Low-Temperature *in Situ* Large-Strain Plasticity of Silicon Nanowires. *Adv. Mater.* **2007**, *19*, 2112–2118.
31. Zhang, Z. Y.; Jin, C. H.; Liang, X. L.; Chen, Q.; Peng, L. M. Current-Voltage Characteristics and Parameter Retrieval of Semiconducting Nanowires. *Appl. Phys. Lett.* **2006**, *89*, 037701.